Nanoscale Advances

ROYAL SOCIETY OF CHEMISTRY

COMMUNICATION

View Article Online
View Journal | View Issue

Cite this: *Nanoscale Adv.*, 2021, **3**, 2777

Received 4th February 2021
Accepted 1st April 2021

DOI: 10.1039/d1na00089f

rsc.li/nanoscale-advances

Orientational self-assembly of nanoparticles in nematic droplets

Natália Tomašovičová, *[a] Marianna Batkova, [a] Ivan Batko,†[a] Veronika Lacková, [a] Vlasta Zavišová, [a] Peter Kopčanský, [a] Jan Jadżyn,[b] Péter Salamon [c] and Tibor Tóth-Katona *[c]

We demonstrate experimentally that the anchoring of a nematic liquid crystal on a solid substrate together with the anchoring of the liquid crystal on a nanoparticle surface induces orientational self-assembly of anisometric nanoparticles in liquid crystal droplets. The observed phenomenon opens a novel route for fabrication of thin colloidal films with tailored properties.

A novel class of soft materials, namely nano- or microparticle dispersions in nematic liquid crystals (LCs), often called LC colloids, are expected not only to provide a fundamental understanding of self-assembly in complex fluids, but also to contribute to the advancement of various fields with tremendous application potential, such as in soft matter physics, materials engineering, nanoscience, and photonics.[1–3] The anchoring of LC molecules at the particle surface combines with the anisotropic elastic properties of the LC matrix to produce distortions in the local molecular orientation field (director) around particles. This leads to new inter-particle forces and new particle ordering behaviours, novel phases and colloidal assemblies in liquid crystals.

Numerous studies have been performed focusing on the theoretical description of the preferred anchoring of LC molecules on the surface of particles.[4–9] Direct experimental observations on the orientation of the particles in respect of the LC matrix are much less common, and the results are somewhat contradicting. For example, 0.5 μm long γ-Fe_2O3 rod-like particles dispersed in nematic *n*-(4-methoxybenzylidene)-4-butylaniline (MBBA) were reported to have a tendency to orient themselves perpendicular to the nematic director.[10] In contrast, single- and multiwalled carbon nanotubes having similar shapes and sizes were found to have parallel orientation to the director in different cyanobiphenyl-type nematic LCs.[11] Obviously, the orientation of the particles is not determined exclusively by their shape.

All the above studies have considered particles embedded in the bulk LC matrix, except ref. 11 in which the LC matrix has been used only for orienting the particles, and the LC has drained through the supporting porous membrane prior to the orientation of particles, which is detected by atomic force microscopy (AFM) measurements. The work presented here is, to our knowledge, the first direct observation of the orientational self-assembly of nanoparticles (NPs) in nematic sessile droplets.

Rod-like iron oxide nanoparticles were synthesized through smooth decomposition of urea[12] and were coated with oleic acid as a surfactant to suppress their aggregation. The morphology and size distribution of the NPs were determined by transmission electron microscopy (TEM): a mean length of 240 nm and mean diameter of 11 nm were found.[13] The well-known thermotropic nematic LCs, 4-(*trans*-4′-*n*-hexylcyclohexyl)-isothiocyanatobenzene (6CHBT),[14] 4-*n*-hexyl-4-cyanobiphenyl (6CB),[15] and their 50 : 50 vol% mixture were used as solvents. Doping the LCs was done by adding the particles suspended in a solvent to the LC in its isotropic phase under continuous stirring and waiting till the solvent evaporates. The resulting volume fraction of the particles in LCs was $\leq 5 \times 10^{-5}$.

For the AFM visualization, the LC colloids were dropped on freshly cleaved mica substrates (PELCO Mica Sheets Grade V5, 15 × 15 mm^2) and spin-coated with the aim to obtain a thin layer of the sample. According to our observations, droplets of different sizes and shapes were formed from the spin-coated thin layer of the LC colloid on the time scale of the order of ~10 minutes. AFM scans on these droplets were carried out using an Agilent 5500 AFM system equipped with PicoView 1.14.3 control software. The images were acquired in the non-contact mode using standard silicon cantilevers (Olympus, model OMCL-AC 160TS) with a resonant frequency of 300 kHz

[a]*Institute of Experimental Physics, Slovak Academy of Sciences, Watsonová 47, 04001 Košice, Slovakia. E-mail: nhudak@saske.sk*

[b]*Institute of Molecular Physics, Polish Academy of Sciences, 16 Smoluchowskiego str., 60179 Poznan, Poland*

[c]*Institute for Solid State Physics and Optics, Wigner Research Centre for Physics, Konkoly-Thege Miklós út 29-33, H-1121, Budapest, Hungary. E-mail: tothkatona.tibor@wigner.hu*

† This communication is dedicated to the memory of the late Ivan Batko.

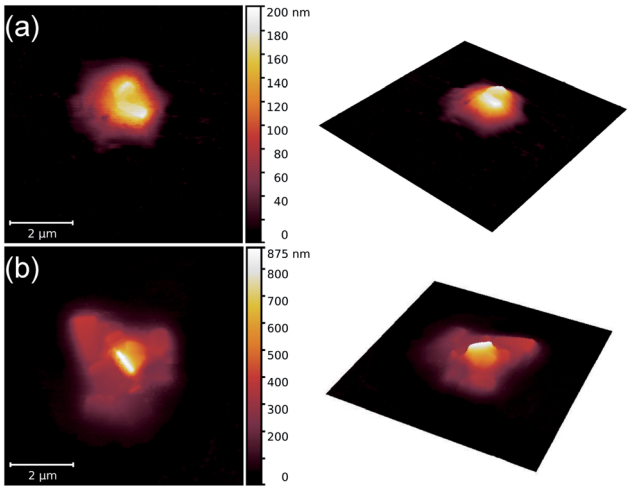

Fig. 1 AFM images illustrating the orientational self-assembly of nanoparticles in two droplets [(a) and (b)] of the 6CHBT nematic liquid crystal.

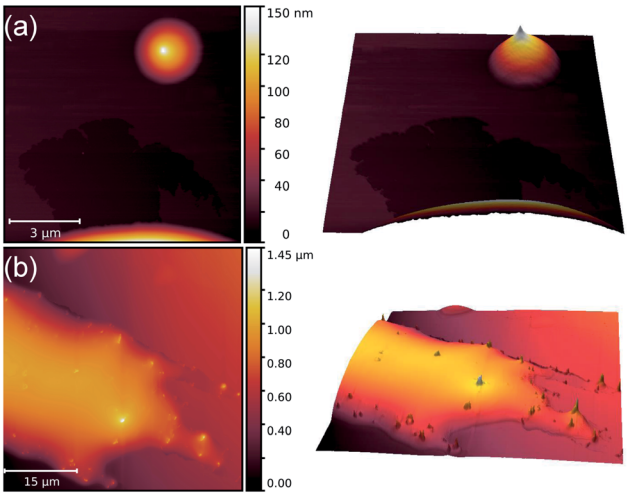

Fig. 3 AFM images illustrating the orientational self-assembly of nanoparticles in two nematic liquid crystal droplets [(a) and (b)] of the 6CHBT and 6CB mixture.

(typ.) and spring constant of 26 N m^{-1} (typ.). The measurements were performed at ambient relative humidity of 30–40%. Using the temperature-controlled sample plate, the temperature was kept at 26 °C during the measurements.

Fig. 1 shows AFM scans for two droplets of 6CHBT with NPs. Clearly, the long axis of the NPs is parallel to the mica substrate.

In Fig. 2 AFM scans on two droplets of the 6CB-NP colloidal system are shown. Although an intense aggregation of NPs is detected in this case, the AFM images indicate their orientational self-assembly to a great extent with the long axis of NPs perpendicular to the mica surface.

In an attempt to resolve the problem of the dissimilar results obtained in 6CHBT and 6CB regarding the orientational self-assembly of NPs, the LC colloidal system of NPs in the 50 : 50 vol% mixture of 6CHBT and 6CB has also been investigated. Fig. 3 shows two AFM scans on the NP orientational self-assembly in the droplets of this mixture. Obviously, the long axis of the NPs is again oriented perpendicular to the mica substrate.

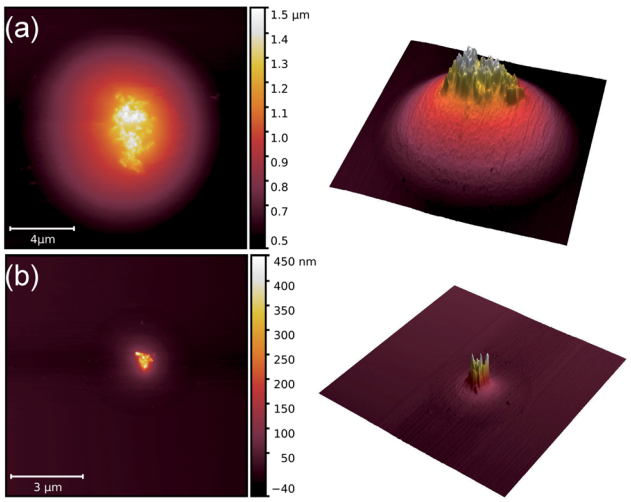

Fig. 2 AFM images illustrating the orientational self-assembly of nanoparticles in two droplets [(a) and (b)] of the 6CB nematic liquid crystal.

Let us consider the interaction between LC molecules and NPs. The type of anchoring at the LC–NP interface has been determined previously by the use of combined electric and magnetic fields. It has been found that the anchoring of LC molecules at the NP surface is planar in both 6CHBT and 6CB LC matrices [*i.e.*, with the nematic director n (describing the average direction of the long LC molecular axis) parallel to the long axis of the particles].[12,16] A rough estimate has also been deduced from these measurements for the anchoring energy density: $\sim 10^{-2}$ N m^{-1} (strong anchoring) for 6CHBT[12] and $\sim 10^{-8}$ N m^{-1} (weak anchoring) for 6CB.[16] Therefore, the above-described AFM observations are surprising: having the same orientation of n at the surface of NPs for both 6CHBT and 6CB LCs, the different orientations of NPs in 6CHBT and 6CB colloidal droplets obviously cannot be explained by the anchoring at the LC–NP interface exclusively. Therefore, the orientation of n on the supporting mica substrate has also been analysed.

Liquid crystal droplets have been deposited on the mica surface with a custom-made apparatus, with which droplets having a lateral size of ~100 μm have been produced (see Fig. 4). The samples are allowed to reach equilibrium for about an hour, after which the mica substrate with the LC droplets is placed under a polarizing optical microscope (POM) working in transmission mode with a monochromatic (red at 660 ± 5 nm) light source. To compensate for the birefringence of the mica substrate, a liquid crystal device (cell) has been introduced in the optical path, the birefringence of which could be regulated by electric field.

Fig. 5 shows POM images of nematic liquid crystal droplets formed by various LCs, under crossed polarizers on the mica substrate compensated for its birefringence. All measurements have been performed at room temperature (≈25 °C).

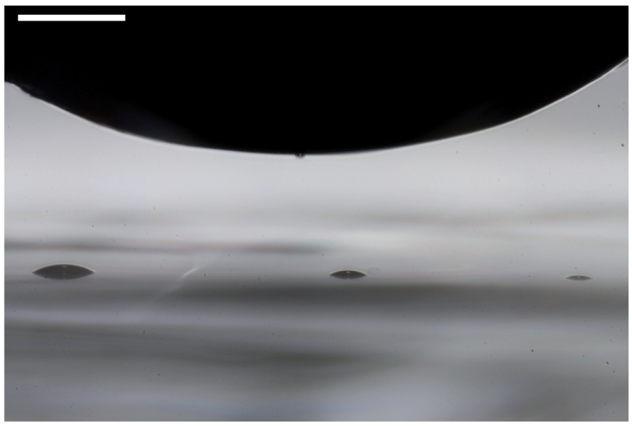

Fig. 4 Deposition of nematic liquid crystal droplets on the mica substrate using a polytetrafluoroethylene rod. The scale bar in the upper left corner denotes 500 μm.

In the case of 6CHBT droplets [Fig. 5(a)], the compensated POM observations clearly indicate the planar anchoring at the mica substrate (*i.e.*, n is parallel to the surface of the substrate) and homeotropic anchoring at the 6CHBT–air interface (n perpendicular to the interface). Namely, Fig. 5(a) strongly resembles the result obtained on droplets of a cyanobiphenyl LC mixture, E7, on a rubbed polyimide substrate.[17] The alignment imposed by the top (air) and bottom (mica) surfaces results in a splay director profile across the droplet. In Fig. 5(a), a disclination line is also visible which results from the topologically incompatible interface between the two oppositely oriented splay director alignments, as illustrated in Fig. 2(d) of ref. 17.

In contrast, the compensated POM observations on 6CB droplets [Fig. 5(b)] indicate homeotropic anchoring both at the mica substrate and at the 6CB–air interface. Namely, the POM images of 6CB droplets consist of four bright parts, with a dark region in the middle. This corresponds to the homeotropic orientation of the LC director at both the mica and air surfaces without defects.[18] This observation is rather surprising considering previous results on 5CB droplets on the mica substrate.[19] 5CB belongs to the same cyanobiphenyl homologous series as 6CB, just having a shorter alkyl-chain with a methylene group. In spite of this minor difference, a planar anchoring of 5CB has been detected on the mica substrate.[19] To confirm this result, we have also analysed 5CB droplets. Fig. 5(c) clearly shows that 5CB droplets have the same properties as the 6CHBT droplets: planar anchoring at the mica substrate and homeotropic anchoring at the 5CB–air interface. Resolving this distinct difference between 5CB and 6CB in the anchoring properties at the mica surface remains for future studies.

The anchoring properties of the 50 : 50 vol% 6CHBT–6CB mixture are less unambiguous than those of 6CHBT and 6CB (or 5CB). However, droplets of the mixture have a clear tendency towards the homeotropic orientation at the interface with the mica substrate as shown in Fig. 5(d) (especially for the droplet having a larger lateral size).

In order to support our conclusions on the director structures in droplets in the case of substrates with different director

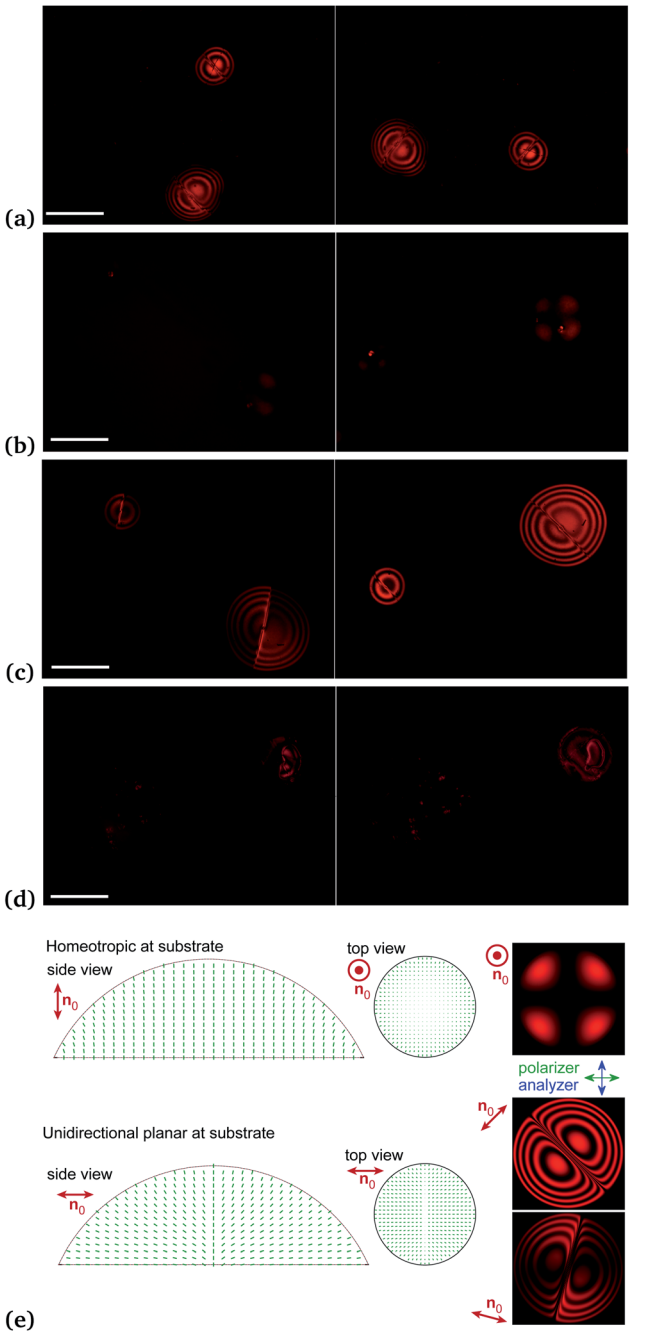

Fig. 5 Nematic liquid crystal droplets under crossed polarizers on the mica substrate compensated for its birefringence. The two images for each LC have been obtained by rotating the microscope stage. (a) 6CHBT, (b) 6CB, (c) 5CB, and (d) a mixture of 6CB and 6CHBT (50 : 50 vol%). The scale bar for each LC sample denotes 500 μm. (e) Cross-sections of the assumed director structures for homeotropic and planar substrates, and the corresponding simulated droplet textures.

alignments (n_0), we performed optical simulations (Fig. 5(e)) based on the assumed director structures, using the Jones matrix method.[20,21] In the homeotropic case, where n_0 is perpendicular to the substrate, the four bright patches are the result of the director tilt due to the curvature near the

circumference of the droplet, when the alignment is also homeotropic at the interface with air. The resulting birefringence leads to increased transmitted intensity in the diagonal directions with respect to the crossed polarizers (see Fig. 5(b) and (e)). If the curvature is low (low contact angle, see Fig. 5(d)), then the four patches are barely visible and may be indistinguishable from the background.

In the case of the planar substrate, we assumed unidirectional n_0 in the plane of the substrate. The different tilt directions on the opposing sides of the droplet lead to a defect line in the middle with a finite width. The presence of the defect line as well as the much larger (multiple orders of) birefringence makes the distinction between the homeotropic and planar cases easy. In the simulations of textures we used the refractive indices of 5CB ($n_e = 1.71$ and $n_o = 1.53$) and the following parameters: drop diameter of 500 μm, contact angle of 17°, defect width parameter of 10 μm, and light wavelength of 660 nm.

Combining the previous knowledge on the anchoring at the LC–NP interface[12,16] with the results presented here regarding the anchoring properties of the LC droplets, the orientational self-assembly of NPs in the LC colloids detected by the AFM measurements can be explained qualitatively.

In the case of NPs dispersed in 6CHBT, the strong anchoring of n parallel to the long axis of NPs,[12] together with the planar anchoring of 6CHBT molecules at the mica surface, results in an orientation of the long axis of the particles parallel to the substrate. The determination of the orientational distribution of the long axis of the particles within the plane of the substrate remains for future studies. Namely, POM images on the 6CHBT droplets in Fig. 5(a) suggest rather a unidirectional orientation of n [*cf.* Fig. 5(a) and 2(b)(i) of ref. 17] than an in-plane axial distribution detected in ref. 19. However, the in-plane misalignment of the long axis of NPs in Fig. 1(a) allows for an in-plane axial distribution suggested by ref. 19.

In 6CB-based LC colloids, the anchoring of n parallel to the long axis of NPs,[16] together with the homeotropic anchoring of 6CB molecules at the mica surface [Fig. 5(b)], results in a robust orientational self-assembly of the long axis of the particles perpendicular to the substrate.

Both constituents of the 6CHBT–6CB mixture exhibit an anchoring at the surface of the nanoparticles such that n is parallel to the long axis of the particles. Therefore, it is expected that the LC mixture has the same anchoring properties as its constituents. Together with the tendency for homeotropic anchoring at the mica substrate [Fig. 5(d)], the mixture-based LC colloid results in the orientation of the long axis of the particles perpendicular to the mica substrate (Fig. 3).

The observed phenomena reported here not only contribute to the fundamental understanding of self-assembly in complex fluids, but may also have a significant technological impact. Namely, the orientational self-assembly of the particles seems to be the consequence of the interplay between the anchoring properties at the LC–NP interface and at the substrate–LC interface. We believe that the anchoring properties at the LC–NP interface primarily depend on the LC material and on the material with which the particles are coated, and not on the material of the NP itself. Therefore, a similar orientational self-assembly of the anisometric particles should not be limited to iron oxide particles. Similarly, in principle, the mica substrate can also be replaced by any other substrate coated with an aligning layer.

Without attempting to be comprehensive, we list some elements of the system potentially worthwhile for future studies. Regarding the nanoparticles, besides metallic, semiconducting, silica, magnetic, or ferroelectric NPs which have already been studied in the bulk LC host (see *e.g.*, ref. 1 and references therein), the orientational self-assembly of Janus NPs[22–24] may also have application potential. As for the particle coating, the oleic acid used in this work can also be replaced. The most promising strategy in this respect is presumably the synthesis of liquid-crystal–nanoparticle hybrids[25] because these hybrids fit the LC host the best. Applicable aligning layers on various substrates range from traditional aligning layers like rubbed polyimide for planar anchoring or DMOAP[26] for homeotropic anchoring, to more special ones, such as CYTOP (exhibiting a temperature induced anchoring transition)[27] or photo-responsive layers.[28] Moreover, eventual replacement of 6CB and 6CHBT LCs with other LC matrices (like 5CB, or the use of 6CHBT and 6CB mixtures in concentrations other than 50 : 50 vol%) further broadens the possibilities for future studies on the effect reported here.

We are confident that using some of the strategies briefly discussed above can lead to fabrication of thin colloidal films with tailored properties based on the observations on orientational self-assembly of NPs described here. In principle, in these envisioned colloidal films, the physical properties [mechanical (*e.g.*, roughness), optical, magnetic, or electric] can be either tuned by external (optical, electric, or magnetic) fields, or can be made final, *e.g.*, by polymerizing the film.

Author contributions

NT – planning and coordination, MB and IB – AFM measurements and analysis, VL – sample preparation, VZ – synthesis of magnetic particles, JJ – resources, PK – funding acquisition, PS – measurements and simulations of LC droplets, and TT-K – planning, coordination and writing. All authors discussed the results, read and approved the final manuscript.

Conflicts of interest

There are no conflicts to declare.

Acknowledgements

The work is supported by the Slovak Academy of Sciences, in the framework of projects VEGA 2/0016/17 and 2/0043/21, and the Slovak Research and Development Agency under contract No. APVV-015-0453. PS and TT-K acknowledge the financial support from the National Research Development and Innovation Office (NKFIH; grant number FK 125134). The authors acknowledge fruitful discussions with Nándor Éber.

Notes and references

1 J. P. Lagerwall and G. Scalia, *Curr. Appl. Phys.*, 2012, **12**, 1387–1412.
2 I. Muševič, *Materials*, 2017, **11**, 24.
3 I. I. Smalyukh, *Annu. Rev. Condens. Matter Phys.*, 2018, **9**, 207–226.
4 S. V. Burylov and Y. L. Raikher, *Phys. Rev. E: Stat. Phys., Plasmas, Fluids, Relat. Interdiscip. Top.*, 1994, **50**, 358–367.
5 O. Kuksenok, R. Ruhwandl, S. Shiyanovskii and E. Terentjev, *Phys. Rev. E: Stat. Phys., Plasmas, Fluids, Relat. Interdiscip. Top.*, 1996, **54**, 5198–5203.
6 R. Ruhwandl and E. Terentjev, *Phys. Rev. E: Stat. Phys., Plasmas, Fluids, Relat. Interdiscip. Top.*, 1997, **56**, 5561–5565.
7 H. Stark, *Eur. Phys. J. B*, 1999, **10**, 311–321.
8 R. Yamamoto, *Phys. Rev. Lett.*, 2001, **87**, 075502.
9 J. I. Fukuda and H. Yokoyama, *Phys. Rev. Lett.*, 2005, **94**, 148301.
10 S.-H. Chen and N. Amer, *Phys. Rev. Lett.*, 1983, **51**, 2298–2301.
11 M. D. Lynch and D. L. Patrick, *Nano Lett.*, 2002, **2**, 1197–1201.
12 P. Kopčanský, N. Tomašovičová, M. Koneracká, V. Zavišová, M. Timko, A. Džarová, A. Šprincová, N. Éber, K. Fodor-Csorba, T. Tóth-Katona, A. Vajda and J. Jadzyn, *Phys. Rev. E: Stat., Nonlinear, Soft Matter Phys.*, 2008, **78**, 011702.
13 V. Gdovinová, N. Tomašovičová, N. Éber, T. Tóth-Katona, V. Zavišová, M. Timko and P. Kopčanský, *Liq. Cryst.*, 2014, **41**, 1773–1777.
14 R. Dabrowski, J. Dziaduszek and T. Szczuciński, *Mol. Cryst. Liq. Cryst.*, 1985, **124**, 241–257.
15 G. Gray, K. Harrison and J. Nash, *Electron. Lett.*, 1973, **9**, 130–131.
16 V. Gdovinová, N. Tomašovičová, V. Zavišová, N. Éber, T. Tóth-Katona, F. Royer, D. Jamon, J. Jadzyn and P. Kopčanský, *Acta Phys. Pol., A*, 2017, **131**, 934–936.
17 E. Parry, D.-J. Kim, A. A. Castrejón-Pita, S. J. Elston and S. M. Morris, *Opt. Mater.*, 2018, **80**, 71–76.
18 S. Shvetsov, A. Emelyanenko, M. Bugakov, N. Boiko and J.-H. Liu, *Polym. Sci., Ser. C*, 2018, **60**, 72–77.
19 L. Blinov and A. Sonin, *Mol. Cryst. Liq. Cryst.*, 1990, **179**, 13–25.
20 R. C. Jones, *J. Opt. Soc. Am.*, 1941, **31**, 488–493.
21 E. Hecht, *Optics*, Addison Wesley, San Francisco, 2002.
22 K.-H. Roh, D. C. Martin and J. Lahann, *Nat. Mater.*, 2005, **4**, 759–763.
23 J. Du and R. K. O'Reilly, *Chem. Soc. Rev.*, 2011, **40**, 2402–2416.
24 J.-B. Fan, Y. Song, H. Liu, Z. Lu, F. Zhang, H. Liu, J. Meng, L. Gu, S. Wang and L. Jiang, *Sci. Adv.*, 2017, **3**, e1603203.
25 G. L. Nealon, R. Greget, C. Dominguez, Z. T. Nagy, D. Guillon, J.-L. Gallani and B. Donnio, *Beilstein J. Org. Chem.*, 2012, **8**, 349–370.
26 M. Škarabot, E. Osmanagič and I. Muševič, *Liq. Cryst.*, 2007, **33**, 581–585.
27 M. Uehara, S. Aya, F. Araoka, K. Ishikawa, H. Takezoe and J. Morikawa, *ChemPhysChem*, 2014, **15**, 1452–1456.
28 A. R. Nassrah, I. Jánossy and T. Tóth-Katona, *J. Mol. Liq.*, 2020, **312**, 113309.